Target Organ Toxicology Series

Toxicology of the Lung

Editors

Donald E. Gardner, Ph.D., D.ATS

Scientific Advisor
Northrop Services, Inc.
Environmental Sciences
Research Triangle Park, North Carolina

James D. Crapo, M.D.

Professor of Medicine
Chief, Division of Allergy,
Critical Care and
Respiratory Medicine
Department of Medicine
Duke University Medical Center
Durham, North Carolina

Edward J. Massaro, Ph.D.

Senior Research Scientist
Developmental and
Cell Toxicology Division
Health Effects Research Laboratory
U.S. Environmental Protection Agency
Research Triangle Park, North Carolina

1988

Raven Press New York

Toxicology of the Lung, edited by
D. E. Gardner, J. D. Crapo, and E. J. Massaro.
Raven Press, New York © 1988.

Absorption of Inhaled Reactive Gases

John H. Overton and Frederick J. Miller

Inhalation Toxicology Division, Health Effects Research Laboratory,
U.S. Environmental Protection Agency,
Research Triangle Park, North Carolina 27711

Dosimetry is an integral component of hazard evaluation for inhaled chemicals. In making interspecies comparisons of toxicological results, dosimetry data allow concentration–response data to be evaluated with respect to dose–response relationships. Thus, knowledge of interspecies differences in dosimetry is critical to the overall risk assessment process.

Dosimetry refers to estimating or measuring the amount of a chemical reaching various target sites. Both experimental and theoretical studies are used in obtaining absorption data for specific chemicals. In this chapter we discuss the uptake of highly reactive gases in the respiratory tract, with emphasis on the physical, chemical, and biological factors involved in absorption and on examples of results of theoretical and experimental dosimetry investigations. The reader is referred elsewhere for treatments of insoluble particles (72), hygroscopic particles (42), and soluble but nonreactive gases (23).

First discussed are the factors and processes that affect the absorption of reactive gases, including the morphological and structural aspects, and the physical and chemical factors involved. The factors discussed are biochemical composition, chemical reactions, solubility, molecular diffusion, and convection in respiratory tract fluids. (For a discussion of transport in the lumens of the airways and airspaces, see ref. 57.) A brief summary of dosimetry experiments involving the uptake of either formaldehyde, ozone (O_3), or nitrogen dioxide (NO_2) by laboratory animals and humans follows. Theoretical dosimetry predictions are considered, with illustrations of the predicted uptake and distribution of O_3 in the lower respiratory tract (LRT) of humans and laboratory animals that resulted from using the models of Miller et al. (48) and Overton et al. (58). The discussion illustrates how theoretical models can be used to explore the effects on predictions from the values of various parameters that characterize the respiratory tract of an animal or species. (For a discussion of the specific mathematical dosimetry model formulation see refs. 47–49,58,59.)

FACTORS AND PROCESSES AFFECTING ABSORPTION

Major factors affecting the local uptake of a reactive gas in the respiratory tract (RT) and RT morphology and anatomy, the route of breathing (nasal, oral, oronasal), the depth and rate of breathing, the physicochemical properties of the gas, the processes of gas transport, and the physicochemical properties of the liquid lining of the lung, lung tissue, and capillary blood. These factors and processes interact in a complex way and must be considered in developing theoretical dosimetry models and interpreting experimental data.

Morphological Aspects

Figure 1 illustrates some of the important aspects of lower respiratory tract (LRT) structures and their relationship to concepts used in modeling. Figure 1a shows a representation, developed by Weibel (80), of the structure of the airways of the tracheobronchial (TB; region distal to but including trachea) region and of the ducts and sacs of the pulmonary region of the human lung. For mathematical modeling, the respiratory tract can be conceived of as a series of sets of right circular cylinders (Fig. 2). Although very simplistic, anatomical models of this type have been found to be useful for simulating the absorption of gases as well as of aerosols. Data are needed on the lengths, diameters, and number of cylinders (that represent the lumens of the airways, ducts or sacs) in each generation, or set. In the pulmonary region, data on the number of alveoli, their surface area and volume are also needed. Table 1 illustrates a typical anatomical model.

In the upper respiratory tract (URT; region proximal to trachea) and in the TB region, the mucociliary layer protects the tissue from direct exposure to the inhaled gas. This layer is composed of an epiphase and an underlying hypophase (Fig. 1c). The epiphase is a highly viscous mucous layer of varying thickness and may not be continuous. At present, this is an area in which most data from animal studies are available. Table 2 gives an indication of some of the thickness data, including animal species studied, location in the respiratory tract where measurements were made, thickness, and relevant comments by the investigators. For humans, data are very limited, and assumptions about the thickness of the liquid lining must be made often based on nonhuman data.

The hypophase is made up of a watery fluid, 4 to 7 μm thick, in which cilia move back and forth in a manner that propels the mucus to the glottis, where it is removed from the respiratory tract along with any collected contaminants on its surface or embedded within. This process is called "mucociliary clearance" and is an important RT defense mechanism.

For irreversible and highly reactive gases, such as O_3, penetration to capillary blood in the URT and TB regions can be ignored (48). Figure 1e illustrates the model compartment concept for this case as well as for the case for which the two liquid phases are assumed indistinguishable. For highly soluble or slowly reacting

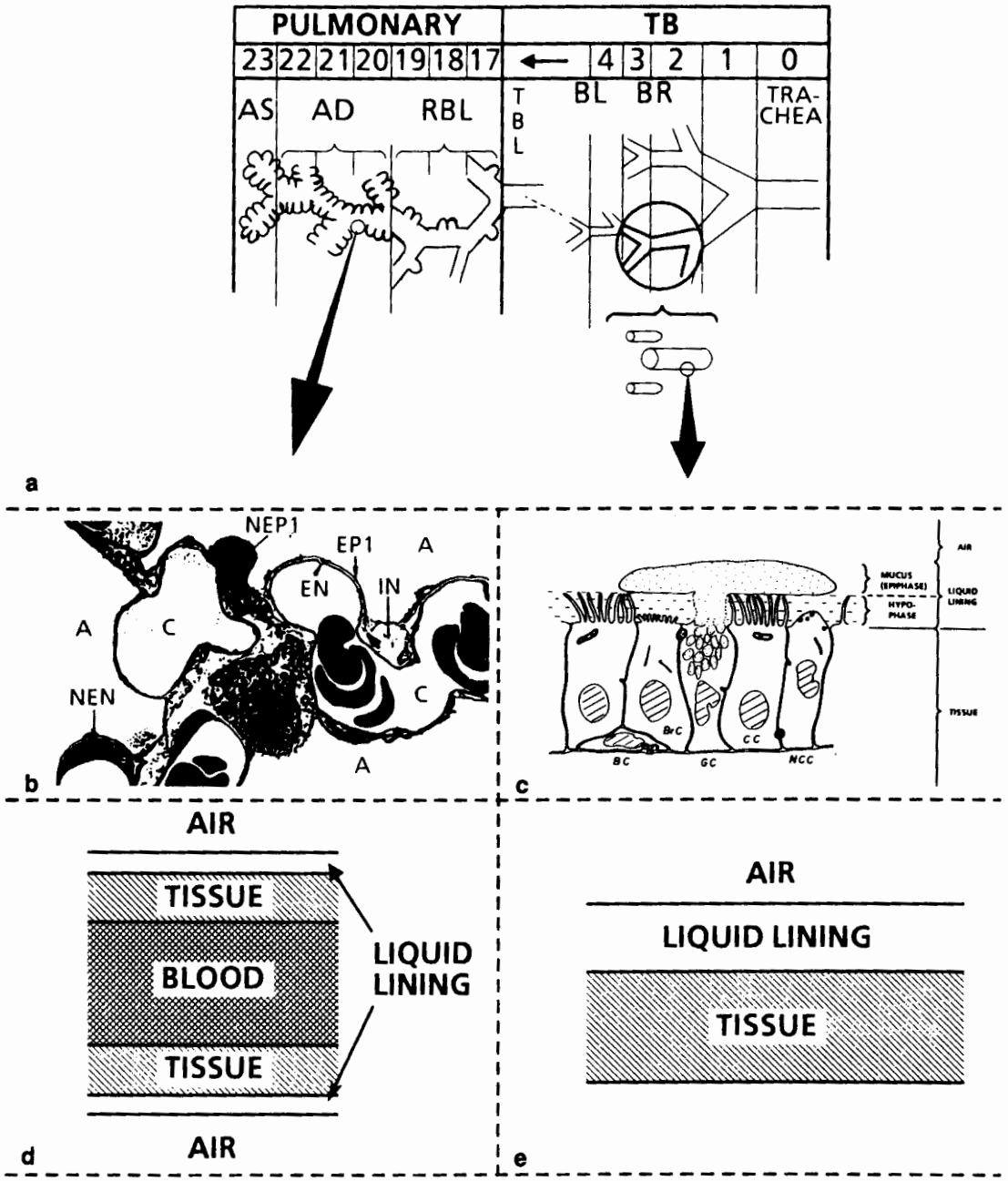

FIG. 1. The relationships between morphologies and their model representations. **a**: Schematic of the branching airways of the tracheobronchial region (TB) and pulmonary region of humans. The generations are labeled from the right, beginning with the trachea. BR, BL, and TBL indicate bronchi, bronchioles, and terminal bronchioles, respectively; the respiratory bronchioles, alveolar ducts, and alveolar sacs are indicated by RBL, AD, and AS, respectively. Below the TB portion of the lung schematic are three cylindrical figures that indicate the model representation of the airways. **b**: Electron micrograph of the interalveolar septa. The air spaces (A), capillaries (C), type I cells and their nuclei (EP1 and NEP1), endothelial cells and their nuclei (EN and NEN), and interstitial space (IN) are indicated. **c**: Diagram of the structure of the liquid lining and tissue of the TB region. The different cells represented are basal (BC), ciliated (CC), brush (BrC), goblet (GC), and nonciliated serous (NCC). **d**: Model representation of the liquid lining, tissue, and capillaries of the pulmonary region. **e**: Model representation of TB liquid lining and tissue compartments. (From ref. 49.)

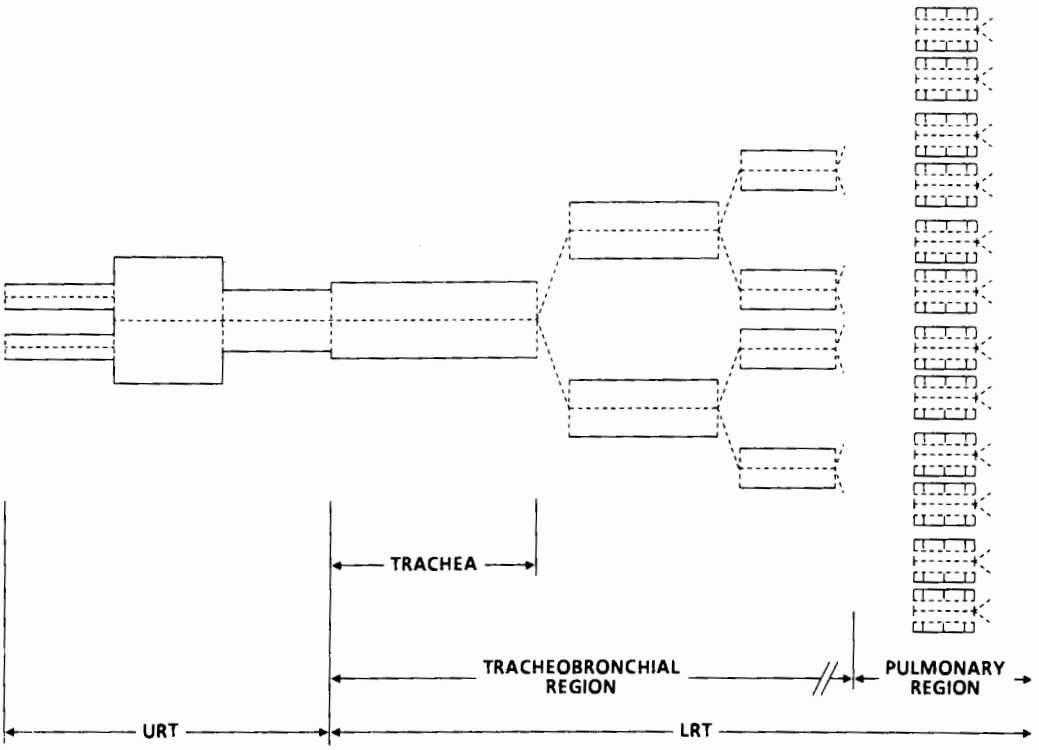

FIG. 2. Diagram illustrating the type of respiratory tract anatomical models used with the dosimetry model.

gases, a blood compartment as well as the consideration of other body organs and compartments may be necessary.

The major features of the pulmonary fluids and tissue structures are illustrated in Fig. 1b. The epithelium is made up predominantly of two types of cells, type I and type II. The first type of cell is identified with the process of respiration; it covers over 95% of the alveolar surface area. Type II cells have metabolic and secretory functions as well as being involved in the repair of damage. A thin liquid film separates the epithelial cells from the air over much of the pulmonary surface area; its thickness is highly variable, from 0.01 to several μm thick, with an average of about 4% of the air–barrier thickness (81). Below the epithelial layer are the interstitium and the wall of the capillaries, the endothelial cells. A simple model formulation for the pulmonary tissue–fluid structure is shown in Figure 1d. Table 3 gives an indication of the type of data available for defining pulmonary tissue and capillary blood compartment dimensions needed in dosimetry models.

Physical and Chemical Aspects

We have been concerned about RT structure and the data necessary to describe the physical dimensions of the airways, ducts, sacs, and alveoli and of the liquid lining, tissue, and capiliary blood compartments. It is within these defined dimensions that the transport of gases occurs and that the chemical reactions of toxic

TABLE 1. *Schematic representation of respiratory tract of guinea pig*[a]

Region	Diameter of duct or alveolus (cm)	Length of duct (cm)	Vol. of duct or alveolus (cm^3)	No. of ducts or alveoli	Alveoli/ duct	Alveoli/ region
Nasal cavity	0.32	2.5	0.48	1		
Nasopharynx	0.30	4.5	0.20	1		
Trachea	0.22	1.2	0.32	1		
1st order bronchi	0.16	1.9	0.042	2		
2nd order bronchi	0.10	0.85	0.037	5		
3rd order bronchi	0.065	0.53	6.6×10^{-3}	17		
4th order bronchi	0.050	0.26	1.8×10^{-3}	86		
5th order bronchi	0.040	0.19	5.1×10^{-4}	312		
6th order bronchi	0.030	0.10	1.9×10^{-4}	1.0×10^{3}		
7th order bronchi	0.023	0.066	7.1×10^{-5}	3.0×10^{3}		
8th order bronchi	0.014	0.045	2.6×10^{-5}	9.5×10^{3}		
9th order bronchi	0.009	0.024	7.0×10^{-6}	4.2×10^{4}		
1st alveolated duct	0.007	0.024	1.6×10^{-6}	1.3×10^{5}	23	2.88×10^{6}
2nd alveolated duct	0.006	0.024	9.2×10^{-7}	2.5×10^{5}	21	5.41×10^{6}
3rd alveolated duct	0.006	0.024	6.8×10^{-7}	5.0×10^{5}	19	9.46×10^{6}
4th alveolated duct	0.005	0.024	6.8×10^{-7}	1.0×10^{6}	19	1.89×10^{7}
5th alveolated duct	0.008	0.032	6.3×10^{-7}	2.0×10^{6}	23	4.55×10^{7}
Alveoli			2.0×10^{-7}	8.2×10^{7}		

[a]From ref. 69.

TABLE 2. *Tracheobronchial and upper respiratory tract liquid lining thicknesses*

Species	Location	Thickness[a] (μm)	Comments	Reference
Rat	Nose	≤15	Observed a continuous blanket	51
Monkey	Nose	Not given	Observed two layers, an "overlying viscid sheet and a layer of serous fluid"	39
Cat	Trachea	≤20; usually <10	Not uniform; "in some areas not detected"	1
Rat	Trachea, large bronchi	5–10	"Distribution was focal"	85
Guinea pig	Trachea	~10	"Constantly biphasic"	31
	Intrapulmonary	0.0	Liquid lining never extended beyond ciliary tips	
Rat	Terminal bronchiole	0.0	No epiphase or mucus observed in healthy rats	32,71
Rabbit	Bronchi (1–3 mm)[b]	5 or more[c]		
	Bronchioles (0.5–1.0 mm)[b]	1–4[c]		
	Bronchioles (<0.5 mm)[b]	0.3–0.5[c]	Mucous blanket observed	40
	Terminal bronchioles	<0.1[c]		

Rat	Trachea	3–15[c], generally 8–12[c]	Mucous blanket observed	41
	Lobar bronchi	Few tenths–8[c], generally 2–5[c]		
Rat	Trachea, major bronchi, peripheral airways		"Well defined streams up to 500 mm wide." "Mucus was transported as discrete particles" as small as 0.5 mm in diameter. A continuous mucous blanket was not observed.	32,75,76

[a]Unless otherwise specified, "thickness" applies only to the epiphase above cilia tips.
[b]Diameter range of airways.
[c]Total liquid lining thickness (epiphase plus hypophase).

TABLE 3. *Alveolar region tissue and blood compartment dimensions of normal mammalian lungs*[a]

	Fischer = 344 rat (n = 4)	Sprague-Dawley rat (n = 8)	Dog (n = 4)	Baboon (n = 5)	Human (n = 8)
Body weight, kg	0.29 ± 0.01[b]	0.36 ± 0.01	16 ± 3	29 ± 3	79 ± 4
Lung volume, ml	8.6 ± 0.31	10.55 ± 0.37	1,322 ± 64	2,393 ± 100	4,341 ± 284
Total volumes, cm^3/both lungs					
A	5.978 ± 0.197	7.216 ± 0.278	914 ± 52	1,851 ± 24	3,422 ± 223
Capillary lumen	0.649 ± 0.057	0.659 ± 0.055	92 ± 5	44 ± 17	169 ± 24
Tissue	0.428 ± 0.046	0.671 ± 0.041	78 ± 4	68 ± 9	314 ± 41
Type I epithelium	0.082 ± 0.006	0.144 ± 0.010	16.5 ± 1.9	14.4 ± 2.3	32.5 ± 3.9
Type II epithelium	0.037 ± 0.009	0.053 ± 0.009	5.6 ± 0.5	3.5 ± 0.8	32.1 ± 5.0
Cellular interstitium	0.068 ± 0.005	0.079 ± 0.015	12.9 ± 0.7	9.4 ± 1.6	54.0 ± 7.0
Noncellular interstitium	0.128 ± 0.016	0.214 ± 0.016	22.8 ± 0.7	24.6 ± 3.7	98.3 ± 12.4
Endothelium	0.094 ± 0.009	0.156 ± 0.007	17.6 ± 1.6	13.4 ± 2.6	42.6 ± 5.4
Macrophages	0.019 ± 0.007	0.025 ± 0.006	2.5 ± 1.1	2.4 ± 1.1	54.7 ± 15.7
Surface area, m^2/both lungs					
Alveolar epithelium					
Type I	0.391 ± 0.039	0.387 ± 0.025	51.0 ± 1.0	47.7 ± 7.7	89.0 ± 8.0
Type II	0.015 ± 0.005	0.015 ± 0.002	1.0 ± 0.2	1.9 ± 0.3	7.0 ± 1.0
Capillary endothelium	0.383 ± 0.039	0.452 ± 0.035	57.0 ± 2.0	38.6 ± 9.5	91.0 ± 9.0
Tissue component of diffusion capacity, ml O_2: min^{-1} mm hg^{-1}	3.43 ± 0.17	3.55 ± 0.33	399 ± 12	23.1 ± 5.2	436 ± 53.6
Tissue thickness, μm					
Harmonic mean, air/plasma	0.379 ± 0.030	0.405 ± 0.017	0.450 ± 0.007	0.674 ± 0.055	0.745 ± 0.059
Arithmetic mean					
Epithelium					
Type I	0.212 ± 0.008	0.384 ± 0.038	0.327 ± 0.043	0.308 ± 0.021	0.361 ± 0.024
Type II	2.758 ± 0.424	3.653 ± 0.266	4.138 ± 0.340	1.839 ± 0.141	5.019 ± 0.551
Interstitium	0.500 ± 0.028	0.693 ± 0.058	0.658 ± 0.033	0.847 ± 0.140	1.634 ± 0.164
Endothelium	0.246 ± 0.011	0.358 ± 0.031	0.308 ± 0.019	0.361 ± 0.038	0.474 ± 0.052

[a]From ref. 12.
[b]All data are mean ± SE.

gases with biochemical constituents take place that may result in toxic effects. In the air phase or air compartment (airway lumens and air spaces), the processes of convection, molecular diffusion, turbulence, dispersion, and the loss or gain of gaseous species to and from the RT walls must be taken into account. The major factors to be considered in lung fluids and tissues include the biochemical constituents of lung tissues and fluids, chemical reactions, solubility, molecular diffusion, convection due to mucociliary action, and capillary blood flow. Transport in the air phase is not discussed here, since it is beyond the scope of this chapter. The reader is refered to Overton (57) for a summary of this topic.

Chemical Composition of Respiratory Tract Fluids and Tissues

Much of what is known about the chemical composition of the liquid lining of the TB region comes from lavage data on patients with pulmonary diseases, such as cystic fibrosis, asthma, and chronic bronchitis. Lavage fluid is separated into two components, the insoluble constituents called "gel" and the solubles in the sol portion. Mucus (gel) has four major constituents: lipids (0.3%–0.5%), glycoprotein (2–3%), proteins (0.1–0.5%), and water (95%). However, the constituents may have been modified from those of healthy people due to disease. The watery substance (sol) may or may not be chemically similar to the periciliary fluid.

Some of the major unsaturated fatty acids (UFA) and amino acids (AA) and their concentrations found in the constituents of lavage fluids, as well as other lung fluids and tissue, are listed in Tables 4 and 5. These materials can be the target of toxic gases; e.g., both O_3 and NO_2 react with UFAs, and O_3 also reacts with AAs. The values in Tables 4 and 5 are calculated using references data.

Data on the chemical makeup of the liquid lining of the pulmonary region come mainly from analysis of the insoluble fraction of pulmonary lavage material. The soluble portion that may correspond to the hypophase of serous fluid is seldom analyzed. The insoluble component, corresponding to the monolayer of surfactant material, is 10 to 20% protein, 1 to 2% carbohydrates, and 80 to 90% lipid (68). Tables 4 and 5 also list some of the UFA and AA components of the insoluble part of pulmonary lavage fluid and their estimated concentrations. The serous fluid, because of its greater thickness, probably has more influence on gas absorption than the thinner surfactant layer.

The chemical composition of blood and tissue is not much different from that of the liquid lining, mainly water with traces of lipids, glycoproteins, proteins, and smaller molecules. However, the concentrations of the molecular components of some of the major constituents of blood and tissue are very different (Tables 4 and 5).

Chemical Reactions

Theoretically, knowledge of all of the chemical species involved in a chemical reaction, the reaction rates of the reactants, and that of the products is needed to

TABLE 4. *Unsaturated fatty acid composition and concentration[a] of human lung secretions, tissue, and blood*

Fatty acid	Mucus[b]	Surfactant[c]	Lung tissue[d]	Whole blood[e]
16:1	0.0738	0.004	8.08	0.12
18:1	0.657	0.0087	25.0	0.77
18:2	0.20	0.0018	8.2	1.12
18:3	0.0006	0.001		0.036
20:1				0.006
20:2	0.035			
20:3				0.034
20:4		0.0005		0.23
10:5				0.06
22:5				0.02
22:6				0.07

[a] μmole/g wet weight. Omitted values correspond to no or insufficient data.
[b] Data derived using ref. 37.
[c] Data derived using ref. 68.
[d] Data derived using Clements refs. 3, 9; Sanders (1982).
[e] Data derived using refs. 25, 28, 55, 62.

characterize a reacting system for modeling purposes. In practice, however, complete information is not always available; even if reaction rates are known, the products and their formation rates may not be available. This may not be a problem if the products are not of interest and do not react significantly with the known reactants.

There is extensive theoretical and experimental information on the absorption and chemical reaction of gases in thin films (4,14,70) that is applicable to the thin

TABLE 5. *Amino acid concentration[a] and composition of human lung tissue, secretions, and blood*

Amino acid	Lung[b] tissue	Mucus[c]	Surfactant[d]	Whole blood[e]
Cysteine	33	0.8	0.007	19.4
Methionine	23	0.6	0.006	17.0
Tryptophan	17	0.3	<0.001	15.6
Tyrosine	45	1.1	0.016	33.6
Histidine	30	0.7	0.009	78.3
Phenylalanine	51	0.8	0.018	70.8
TOTAL	199	4.3	0.056	234.7

[a] Data are in units of μmoles/g wet weight.
[b] Data derived using refs. 3, 6, 20.
[c] Data derived using refs. 7, 13, 34; Riley and Brogan (1973).
[d] Only the monomolecular surface-active film. Data derived using refs. 60, 67, 68.
[e] Data derived using refs. 6, 21, 35.

layers of the liquid lining, tissues, and capillaries of the lung. Much of this theoretical work deals with simplifying techniques for solving complex problems that involve chemical systems.

The chemistry of absorbed gases in water is important, not only because 85 to 95% of the main constituent of lung fluids and tissues is water but also because many toxic species react with water, affecting the absorption rate, as well as creating products that may be important in further reactions with the absorbed gases and the biological constituents. NO_2, O_3, NH_3, SO_2, and CO_2 are common in the atmosphere and react with, as well as interact in, water (16,17), giving rise to bisulfite, nitrite, nitrate, and sulfate molecules and the potential for lowering pH, all of which could have direct or indirect adverse effect on lung tissues and fluids.

Examples of some of the water reactions are given in Table 6. The reactions of the carbon, sulfur, and nitrogen compounds are interrelated by the hydrogen ion. In addition, O_3 oxidizes both nitrogen and sulfur species. With the introduction of biochemical constituents, the reacting system will become more complex. Depending on conditions, however, some of these reactions will be more important than others. If necessary, the important reactions can be determined by chemical kinetic modeling to gain information that will allow simplifying the system (by keeping only the important reactions) for use in dosimetry modeling.

According to Menzel (43), the most toxic of oxidizing air pollutants is O_3, its oxidative properties being responsible for its toxicity. Thus, as an example of the type of reactions of a toxic gas with biochemical constituents that may have to be considered in developing a dosimetry model, the reactions of O_3 are briefly outlined. Even though O_3 reacts with almost all classes of biological substances, physiological, morphological, and biochemical effects of O_3 point to cellular membranes as the likely site of toxicity (44), suggesting lipids as the major target. Olefins are very sensitive to O_3; the mechanism of reaction is the Criegee mechanism (65), in which O_3 attacks the carbon double bond in the UFA. Other mechanisms also are involved in which toxic free radicals are produced that can cause damage; however, the Criegee process is considered the main reaction path for most O_3–UFA reactions (65).

Rate constants for the reaction of O_3 with some biological UFAs are known (66); nevertheless, for most biological substances, rate constants *in vivo* are lacking; e.g., the degree to which O_3 is able to penetrate membranes and react with the double bonds on UFAs in lipids is unknown (65).

According to Pryor et al. (65) O_3 also reacts with amino acids, proteins, and sugars. In water the only AAs found to react with O_3 are (in order of increasing reactivity) phenylalanine, cystine, hystidine, tyrosine, tryptophan or methionine, and cysteine. The mechanisms for damage to proteins are not well known, but a nonradical Criegee process is possible, and there is evidence for a radical path. Sugar reactions are expected to be slow; however, the reaction of O_3 with sugars, as well as with nucleic acid, has not been studied. Vitamin E is known to protect both UFAs and lung tissue against some of the effects of O_3 by scavenging radicals; even so, vitamin E does not interfere with the nonradical Criegee process.

TABLE 6. *Chemical reaction mechanism of the CO_2–O_3–SO_2 and nitrogen oxide aqueous system*[a]

1. H_2O	$\rightleftarrows$	$H^+ + OH^-$	10. $HNO_2 + HNO_2$	$\rightleftarrows$	$N_2O_3 + H_2O$
2. $CO_2 + H_2O$	$\rightleftarrows$	$H^+ + HCO_3^-$	11. N_2O_3	$\rightleftarrows$	$NO + NO_2$
3. HCO_3^-	$\rightleftarrows$	$OH^- + CO_2$	12. $NH_3 + H^+$	$\rightleftarrows$	NH_4^+
4. $SO_2 + H_2O$	$\rightleftarrows$	$H^+ + HSO_3^-$	13. NH_3	$\rightleftarrows$	$NH_4^+ + OH^-$
5. HSO_3^-	$\rightleftarrows$	$H^+ + SO_3^{2-}$	14. $O_3 + SO_2$	$\rightleftarrows$	$SO_4^{2-} + 2H^+$
6. $NO_2 + NO_2$	$\rightleftarrows$	N_2O_4	15. $O_3 + SO_3^{2-}$	$\rightleftarrows$	SO_4^{2-}
7. $N_2O_4 + H_2O$	$\rightleftarrows$	$HNO_2 + HNO_3$	16. $O_3 + HSO_3^-$	$\rightleftarrows$	$H^+ + SO_4^{2-}$
8. HNO_2	$\rightleftarrows$	$H^+ + NO_2^-$	17. $O_3 + NO_2^-$	$\rightleftarrows$	NO_3^-
9. HNO_3	$\rightleftarrows$	$H^+ + NO_3^-$			

[a]Based on refs. 16, 17.

Solubility

The ability of a medium, such as water, blood, mucus, or tissue, to absorb a gas is called "solubility." There are many different expressions for quantifying the solubility of gases, including Ostwald's, Bunsen's, Kuenen's, and Henry's laws (10). For example, the Bunsen absorption coefficient is defined as the volume of gas at standard temperature and pressure dissolved by unit volume of a liquid when the partial pressure of the gas is 1 atm. Chemical reactions may or may not be involved; thus, not only does Bunsen's coefficient account for total absorption, but also its value depends on the properties of chemical reactions, if any.

As long as the concentration of dissolved gas is small and the pressure and temperature are not close to the critical pressure and temperature, Henry's law is obeyed. This law applies only to the uncombined or free form of the gas in solution; thus, it does not account for all of the absorbed gas. However, Henry's law constant is independent of chemical reactions and can be used in quantifying the concentration of the molecular form of a gas in solution that may be involved in chemical reactions. The law can be expressed in several different, but equivalent, forms for the same gas and liquid, a convenient form being, $C_g = HC_l$. C_g and C_l are the gas and liquid phase concentrations, respectively. H is Henry's law constant, and it is the ratio at equilibrium of the gas phase concentration to the liquid phase concentration of the gas (e.g., moles per liter in air/moles per liter in solution). In general, the constant is a function of temperature and the molecular properties of the liquid and the gas, but for constant temperature and the ranges of ambient concentrations of toxic gases, the coefficient can be considered constant and is applicable to biological systems.

Henry's law is applicable to layers of biological fluids and tissues. In this situation, the ratio at equilibrium of the concentrations in the two phases or layers is the ratio of the Henry's law constant of the air/solution system of one phase to the Henry's law constant of the air/solution system of the other phase. This ratio is called the "distribution coefficient" or the "partition coefficient."

Table 7 is a list of gases and Henry's law constants for water. The gases are listed in order of decreasing values of the constants, with increasing solubility, provided there were no chemical reactions involved. Henry's law constant relates the molecular form of the gas in water and air and not the total quantity absorbed in water to air quantities. Thus, as defined in this latter sense, the relative solubilities of the gases in Table 7 may be different than implied by the order.

In Table 8, a collection of Henry's law constants for several gases in biological fluids and tissues, for the small molecules listed, there is not much variation for Henry's law constant among the various substances for a given gas. Except for C_2H_4, the use of the water value would seem justifiable. Although Table 8 is incomplete, it suggests that the value of H is not influenced much by different biological tissues and liquids, suggesting that a known value for one tissue or liquid is a reasonable approximation for missing values.

TABLE 7. *Henry's law constant for selected gases in water*

Gas	Henry's Law constant[a]	Reference	Major site of toxicity or absorption[b]
Nitrogen (N_2)	77	2	P
Carbon monoxide (CO)	55	2	P
Oxygen (O_2)	42	2	P
Nitrogen oxide (NO)	24	61	TB and P
Ethylene (C_2H_4)	13	2	
Nitrogen dioxide (NO_2)	8.8[c]	36	TB and P
Ozone (O_3)	6.4	Roth and Sullivan (1981)	TB and P
Methane (CH_4)	3.5	61	
Carbonyl sulfide (COS)	2.8	61	
Nitrous oxide (N_2O)	2.4	61	
Carbon dioxide (CO_2)	1.8	2	P
Acetylene (C_2H_2)	1.3	2	
Formaldehyde (HCHO)	0.56	53	URT
Hydrogen sulfide (H_2S)	0.5	61	URT and
Sulfur dioxide (SO_2)	0.048	27	large bronchi
Ammonia (NH_3)	0.0011	61	URT

[a]37°C; (moles/liter/air)/(moles/liter/water).
[b]From ref. 53. (TB) tracheobronchial region; (URT) upper respiratory tract; (P) pulmonary region.
[c]Extrapolation to 37°C based on the temperature dependence of ozone.

A list of partition coefficients for small molecule gases with several biological tissues and fluids is given by Altman and Dittmer (2). The values are close to one suggesting that animal fluids and tissues are very similar as far as solubility of gases of small molecules is concerned, further supporting the conclusion in the preceding paragraph. This does not hold in general, however, for the gaseous organic compounds, and extrapolation from water data to biological fluids and tissues is not always appropriate.

Molecular Diffusion

Molecular diffusion is a process that redistributes molecules in such a way that there is a net flow of the molecules from regions of high concentration to regions of lower concentration (14). The flux, F, or the net rate of transfer of mass or of the number of specific molecules across a plane perpendicular to a given direction due to molecular diffusion is defined as $F = -D\,(dc/dx)$. In this equation, known as Fick's law, dc/dx is the concentration gradient along the given direction and D is the molecular diffusion coefficient.

The value of the diffusion coefficient depends on the properties of the gas molecule and the medium. Although the effect of polymers on diffusion follows no

TABLE 8. *Henry's law constant for various gases in liquid and tissue*[a]

	Liquid						Tissue				
			Whole blood		Plasma		Heart		Brain		
	Water	Water (0.155 N NaCl)	Human	Dog	Human	Dog	Human	Dog	Human	Dog	Lung (rat)
O_2	42[b]	45	43		48						56
CO_2	1.8	1.9	2.0		1.9						
C_2H_4	13		8.1	7.1							
C_2H_2	1.3		1.4	1.3		1.4					
N_2O			2.4	2.4			2.2	2.2	2.3	2.3	
N_2	77	83									

[a]From ref. 2.
[b]Values are in units of (moles/liter in air) per (moles/liter in solvent).

simple pattern, the diffusion coefficient of small molecules, such as O_2 and CO_2, in solutions of biological proteins is approximately the same as in polymer solutions (54,70). Thus, the diffusion coefficients of small molecules in dilute polymer solutions, with constituents similiar to those in biological fluids and tissues, are probably similar to but smaller than the value in pure water. For small molecules other than O_2 and CO_2, such as O_3 and NO_2, this conclusion probably is reasonable. For the larger gaseous and organic molecules, diffusion coefficients in biological substances may be very different from the pure water values, making measurements in biological tissues and fluids necessary.

Values for the molecular diffusion coefficient of a few gases in biological fluid and tissues have been measured. The values are generally less than in water. According to Altman and Dittmer (2), e.g., the values for O_2 in water, ox serum, frog muscle, dog connective tissue, and rat lung tissue are 3×10^{-5}, 1.7×10^{-5}, 1.2×10^{-5}, $.97 \times 10^{-5}$, and 2.3×10^{-5} cm^2/sec, respectively.

Bulk Flow or Convection in Lung Fluids

The liquid lining of the URT and TB regions and capillary blood are in motion. This motion, or flow, is such that absorbed gases can be redistributed in the RT or even transported to nonlung organs and compartments, to be lost from the RT or possibly to be returned. In addition, depleted biochemical compounds can be replenished by the flow process. The extent of the redistribution depends on the particular flowing system and the reactive gas. Miller et al. (48) estimated that for O_3, an irreversible reacting and highly reactive gas, pulmonary capillary blood flow rates and TB liquid lining or mucous flow rates are too slow to affect O_3 absorption.

To be able to account for liquid flow or convection in modeling, the rates of flow (e.g., volume of liquid per unit time) of the fluids are needed. Mucous flow rates in the URT (51,64) and the larger airways of the TB region (22,32) are available for several species. Iravani and van As (32) reported rates in the smaller airways. In addition, estimates of rates in all airways have been made based on clearance data from selected airways, anatomical data, and other assumptions (46, 74). Transport rates in each airway generation of guinea pigs were estimated by Velasquez and Morrow (78) by applying kinetic equations to data on particle retention in five airway zones (based on airway diameter). The estimated mucociliary (particle) rates ranged from approximately 8 mm/min in the trachea to 0.001 mm/min in the distal bronchioles. However, mucociliary rates are not necessarily the same as the liquid lining bulk or convective flow rates, and further data or assumptions must be used to estimate convection velocities. Nevertheless, the estimated rates are probably a good first approximation.

Pulmonary capillary blood flows have been measured (30,79), as well as theoretically calculated (56,86). Because the distance from the air to capillaries in the TB region is at least 7 to 20 times as great as it is in the pulmonary region, highly but irreversibly reacting gases, such as O_3, will not reach the capillaries proximal

to the pulmonary region (48). However, Heck et al. (29) demonstrated that either formaldehyde (HCHO) or (most probably) its reaction products were transferred to extrapulmonary tissues and fluids outside the URT. NO_2 products are known to be transferred out of the lung (26,63), and probably TB or pulmonary region capillary blood flow is a major factor in the transfer. Thus, in developing dosimetry models, the effect on gas absorption by product removal from the lung and by reintroduction into the RT by blood flow should be considered to determine their importance.

ABSORPTION IN EXPERIMENTAL ANIMALS AND HUMANS

Upper Respiratory Tract Experiments

Formaldehyde

Egle (18) measured the upper respiratory tract uptake of HCHO in dogs. For the two-way experiment in which air was passed through the URT "in a manner as to represent both inhalation and exhalation" (18), 100% of the HCHO was retained at all flow rates. In the one-way experiments (simulating inhalation), the uptake increased from 95% to 100%, with increasing flow rate.

The investigation of Heck et al. (29) was concerned with the distribution of inhaled $H^{14}CHO$ in different tissues and fluids of rats. The highest concentrations of radioactivity were observed in the nasal mucosa of the URT. Radioactivity was detected also in lung tissue and in nonlung tissue, indicating rapid transfer of $H^{14}CHO$ or reaction products out of the respiratory tract. For the 6 hr exposure, the amount absorbed was found to be approximately proportional to the air concentration.

Swenberg et al. (73) used $H^{14}CHO$ and autoradiography to locate the regions of high deposition in the URTs of rats and mice. They found heavy deposition of radioactivity in the anterior nasal cavities, correlating well with observed lesions in similarly exposed animals. Heavy deposition was found also in the ventral portion of the cavity, where significantly fewer tumors have been found. This region is lined with squamous epithelium, suggesting less sensitivity of this type of epithelium to HCHO compared to respiratory epithelium. A whole body autoradiograph showed heavy deposition of radioactivity in the nasal cavity and in the anterior half of the trachea. Moderate amounts were deposited in the bronchi. Autoradiography, combined with densitometry, may be useful in determining the relative amounts of radioactivity in different areas or locations of the URT and in the major airways of the LRT.

Ozone

The isolated upper airways of beagle dogs were exposed to O_3 at a continuous flow of 3.0 liters/min by Vaughan et al. (77). For concentrations of 0.2 to 0.4 ppm,

100% uptake by the nasopharyngeal region was reported. Yokoyama and Frank (84) observed 72% uptake at 0.26 to 0.34 ppm (3.5 liters/min to 6.5 liters/min flow rate) using a different procedure. Replicating the procedure of Vaughan et al. (77), Yokoyama and Frank (84) found that O_3 was absorbed on the wall of the mylar bag used in collecting the gas below the trachea, suggesting that the 100% uptake results of Vaughan et al. were the result of experimental artifacts. If only the data for the inspired concentrations from 1 ppm to 9 ppm in the figure in Vaughan et al. (77) are considered, the uptake is 60 to 70%, in keeping with the values reported by Yokoyama and Frank (84) for the much lower concentrations.

Yokoyama and Frank (84) also observed a decrease in the percent uptake due to increased O_3 concentration and due to increased flow. With nasal breathing at approximately 0.3 ppm O_3, the uptake decreased from 72% to 37% for a flow rate increase from 5 to 40 liters/min. An increase in concentration from 0.3 ppm to 0.79 ppm decreased nasal breathing uptake (at 5 liters/min) from 72% to 60%. Their data also indicate that tracheal concentrations increased with increasing oral or nasal concentrations. Also demonstrated was the fact the percent uptake as well as the concentrations of O_3 reaching the trachea depended heavily on the route of breathing. For a given flow rate, nasal uptake significantly exceeded oral uptake.

The loss of O_3 in the URT of acutely and chronically exposed dogs was investigated by Moorman et al. (50). Chronically exposed (18 months) to 1 to 3 ppm of O_3, beagle dogs under various daily exposure regimens had significantly higher tracheal O_3 concentrations than animals tested after 1 day of exposure to similar regimes. The authors suggested that the differences were due to physicochemical changes of the mucosal lining of the chronically exposed animals. Additionally, dogs exposed for 18 months to 1 ppm for 8 hr per day exhibited lower tracheal concentrations than those continuously exposed. However, according to EPA (19), when the insensitivity of the O_3 monitor used to measure the responses is taken into account, the average tracheal concentrations of the acutely and chronically exposed animals are not significantly different. Thus, at the levels of exposure used in the experiment, there is no evidence that chronic exposure would result in lower tracheal concentrations than acute exposure.

Miller et al. (45) studied the nasopharyngeal removal of O_3 in rabbits and guinea pigs over a concentration range of 0.1 ppm to 2.0 ppm. The O_3 concentration in the trachea in the two species was found to be similar for the same inhaled concentration, the tracheal concentration being linearly related to the chamber concentration that was drawn through the isolated upper airways. Ozone removal in both species was approximately 50%.

Gerrity et al. (24) inserted a small polyethylene tube into the nose of human subjects (seated in a chamber into which O_3 was introduced) so that the tip was positioned in the posterior pharnyx. Air was withdrawn at this position and sampled by a rapidly responding O_3 analyzer, resulting in real time measurements of inhaled and exhaled O_3 concentrations. This arrangement allowed for the determination of the absorption efficiencies both proximal and distal to the posterior pharynx. The efficiencies were determined as a function of O_3 concentration (0.1, 0.2, and 0.4

ppm), respiratory frequency (12 and 24 bpm), and breathing mode (mouth only, nose only, and oronasal). The mean O_3 removal efficiency proximal to the posterior pharynx was 39.6 ± 0.7% (SEM). Significantly less O_3 was removed at 24 bpm than at 12 bpm (38.2% and 41.0%, respectively), O_3 concentration had no effect on removal from the upper region, and significantly less O_3 was removed during nasal breathing than during the other two modes (36.0%, 40.0%, and 42.8% for nasal, mouth, and oronasal, respectively).

Lower Respiratory Tract Uptake Experiments

Formaldehyde

HCHO uptake in the lower respiratory tract of dogs was measured by Engle (18). Ninety-five to one hundred percent of the inspired HCHO was retained, the data suggesting that the percent uptake decreased with increased ventilatory rate.

Ozone

Yokoyama and Frank (84) measured the removal of O_3 from inspired air in the ventilated lower respiratory tract of beagle dogs. The uptake was found to vary between 80 and 87%, independent of the two levels of concentration (0.77 ppm and 0.3 ppm) and the two flow rates (20 or 30 breaths/min).

Gerrity et al. (24) measured the absorption efficiencies of the region of the RT distal to the posterior pharynx. The mean absorption efficiency was 91.0 ± 0.5% of the O_3 inhaled through the posterior pharynx. Significantly more O_3 was absorbed at 12 bpm than at 24 bpm (92.6% compared to 89.3%), and significantly less O_3 was removed at 0.1 ppm than at 0.4 ppm (89.4%, 90.9%, and 92.5% for 0.1, 0.2, and 0.4 ppm, respectively). No differences in uptake due to mode of breathing were detected.

Nitrogen Dioxide

Corn et al. (11) determined the average mass transfer coefficient (K) of NO_2 in the LRT of cats. The region of measurement was between the trachea and a portion of the lung associated with the "right lateral thoracic region between the fourth and fifth rib" (11). They reported no change in K as a result of NO_2 concentration changes or ventilatory rate changes. However, NRC (53) claims that the data on K (11) show a square root dependency on frequency. Postlethwait and Mustafa (63) reported the uptake of NO_2 by an isolated perfused rat lung. The isolated lungs were exposed for 90 min to 5 ppm NO_2 at a ventilation rate of 45 ml/min. Thirty-six percent of the ventilated NO_2 was absorbed.

Total Uptake Experiments

Formaldehyde

Experiments were carried out by Egle (18) to determine the total uptake of HCHO in dogs. Retention varied from 95 to 100% regardless of the tidal volume (100–200 ml) or ventilatory rate (8–20 breath/min). However, a slight increase in percent uptake was observed with increasing HCHO concentration.

Ozone

Wiester et al. (82) determined the uptake of O_3 in awake adult rats in a head-out plethysmograph. The rats breathed for 1 hr either 0.3, 0.6, or 1.0 ppm O_3. Of the O_3 inhaled, 40 ± 11% (SD) was retained, independent of time and concentration. Further, the total dose was proportional to concentration.

Nitrogen Dioxide

Adult asthmatics were exposed to 0.3 ppm NO_2 for 30 min by Bauer et al. (5). All exposed subjects inhaled NO_2 by mouthpiece for 20 min at rest, then exercised for 10 min on a bicycle ergometer. The inspired and expired NO_2 concentrations were measured, showing that at rest the uptake was 73 ± 6% (SD), whereas during exercise the uptake was 88 ± 4%, a significant increase. Minute ventilations during the rest and exercise periods were 8.1 liters/min and 30.4 liters/min, respectively; for the same period of time, 4.8 times as much NO_2 was absorbed during exercise as during rest (52).

THEORETICAL PREDICTIONS OF LOWER RESPIRATORY TRACT ABSORPTION OF OZONE IN ANIMALS AND HUMANS

The Effect of Anatomical Models on Distribution of Predicted Absorbed Ozone

The effects of different anatomical models on the distribution and uptake of absorbed O_3 in the LRT of rats and guinea pigs were investigated by Overton et al. (58). Two anatomical models were used for each species. Figure 3 shows the simulated tissue and net dose profiles for the four anatomical models. The doses are plotted versus generation, order, or zone, depending on the particular anatomical model as defined by the original investigators for each model.

The general shape of the curves are independent of ventilatory parameters and illustrate some of the similarities and differences in predictions using the different anatomical models. Generally, the tissue dose is low in the trachea, rising to a

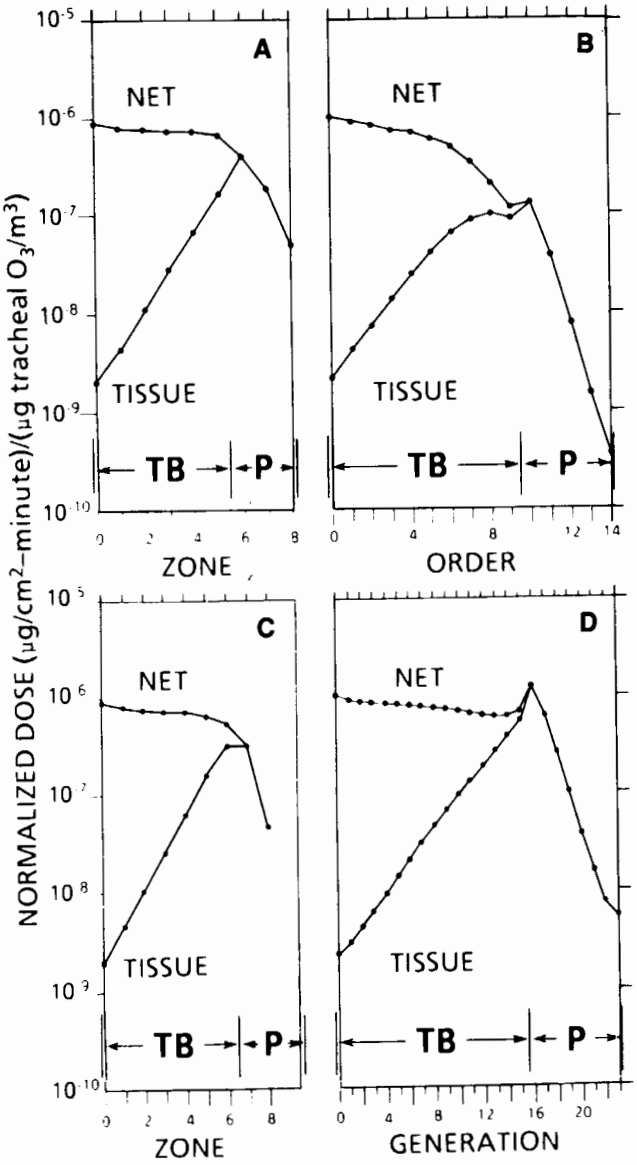

FIG. 3. Effect of four different lower respiratory tract anatomical models on predicted net and tissue ozone (O_3) dose profiles of guinea pig and rat. Dose is the quantity of O_3 reacting with biological constituents per unit surface area of a zone, order, or generation, per unit time per tracheal O_3 concentration. Net dose is the sum of the liquid lining, tissue, and blood compartment doses. **A**: Dose versus zone, Kliment (33) anatomical model for guinea pig, V_T = 2.53 ml, f = 56.6 bpm. **B**: Dose versus order, Schreider and Hutchens (69) anatomical model for guinea pig, V_T = 2.4 ml, f = 77 bpm. **C**: Dose versus zone, Kliment (33) anatomical model for rat, V_T = 0.7 ml, f = 144 bpm. **D**: Dose versus generation, Yeh et al. (83) anatomical model for the rat, V_T = 1.84 ml, f = 105 bpm. (TB) tracheobronchial region (mucus lined); (P) pulmonary region (surfactant lined). Multiply figure values by tracheal concentration (μg/m³) to obtain dose (μg/cm²/min). (From ref. 58.)

maximum value in the vicinity of the centriacinar region. From here and proceeding distally in the pulmonary region, the tissue dose rapidly decreases. Net dose is large in the trachea, decreasing distally to the pulmonary region, where the net dose either rapidly increases or continues to decrease, depending on the anatomical model. Tissue and net dose are approximately the same in the pulmonary region.

The plots resulting from using the Kliment (33) anatomical models of the guinea pig and rat (Fig. 3A, C) are similiar in shape, except at the sixth and seventh zones, where the guinea pig tissue dose peaks in contrast to the rat tissue dose curve that plateaus and then decreases. This difference reflects the choice of where the surfactant-lined or pulmonary region begins. For the guinea pig, the region begins at the sixth zone and for the rat the region begins in the seventh zone. Pulmonary and total uptake for the Kliment rat (Fig. 3C) are 81% and 87%, respectively. For the Kliment (33) guinea pig, the uptakes are 85% and 92%, respectively.

The similarity of rat and guinea pig dose profiles, as predicted by use of the Kliment (33) anatomical models, does not extend to the predictions made by use of the Schreider and Hutchens (69) and the Yeh et al. (83) anatomical models for the guinea pig (Fig. 3B) and rat (Fig. 3D). These two models result in considerable differences; e.g., the net tracheal dose for the rat is smaller than the tissue and net dose of the first alveolated duct. On the other hand, the net dose predicted for the trachea of the guinea pig is approximately seven times larger than the net dose predicted for the first completely alveolated duct of this species. However, the net dose profiles are alike in that they peak in the first alveolated generation or order, a feature not present in the simulations using the anatomical models of Kliment (33).

The intraspecies and interspecies differences in predicted dose profiles (Fig. 3) may be more a result of incorrect or unrepresentative anatomical model characterizations than due to actual differences between or within species. Nevertheless, the results show the importance of anatomical dimensions on predicted absorption in the LRT and the need for correctly specified anatomical models (58).

Effect of Tracheobronchial Liquid Lining Thickness on Predictions

Miller et al. (48) showed that the thickness of the liquid lining of the TB region and the respiratory bronchioles (RB) is critical to the prediction of tissue dose in the TB region. Figure 4 shows the effects of three TB/RB liquid lining thickness schemes on tissue dose using the anatomical model of Weibel (80) for humans. The reference thickness (resulting in curves A and A′) are 10.0, 8.6, and 7.2 μm in generations 0, 1, and 2, respectively. From generation 2 through generation 20, thickness is assumed to decrease linearly with respect to generation index. Generation 20 is the first completely alveolated generation in the Weibel (80) anatomical model. From generation 20 to 23, the liquid lining thickness is assumed to be 0.125 μm. The thickness schemes for curves B/B′ and C/C′ are such that for generations 0 to 19 the B/B′ thicknesses are one-half those of the reference values, and the C/C′ thicknesses are twice those of the reference values. Values of the thicknesses of the three schemes are within the range of reported values (Table 2; note that some of the investigators reported thickness above the hypophase, and others reported the total liquid lining thickness).

The most obvious effect of thickness change is the pronounced decrease in TB tissue dose (curves A, B, C) as the thickness increases, whereas the net doses (curves A′, B′, C′) are hardly affected. In general tracheal tissue dose is very low and is different for the three thicknesses, with more than two orders of magnitude separating the extreme values of tracheal tissue doses. From the trachea, the tissue doses increase distally to a maximum near the terminal bronchioles (generation 16). For the thinnest lining (curve B), the maximum occurs in the 15th generation. Two maximums occur for the reference thickness lining (curve A), one at the 15th and the other at the 17th generation (first respiratory bronchioles). The tissue dose for

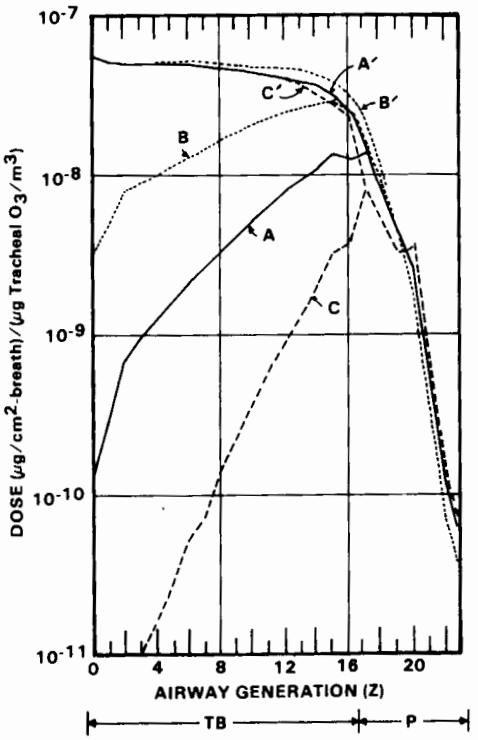

FIG. 4. The effect of liquid compartment thickness schemes on O_3 tissue dose (curves A, B, and C) and on the corresponding net dose (A′, B′, and C′). Curves A and A′: reference curves, thickness scheme A. Curves B and B′: thickness scheme B (one-half thickness of scheme A). Curves C and C¹: thickness scheme C (twice thickness of scheme A). (TB) tracheobronchial region (mucous lined); (P) pulmonary region (surfactant lined). Multiply figure values by tracheal concentration ($\mu g/m^3$) to obtain dose ($\mu g/cm^2$ per breath). (From ref. 48.)

the thickest lining occurs in the first order of respiratory bronchioles. In all three cases, the tissue dose decreases distally from the last maximum to very low values in the pulmonary sacs (generation 23).

The net doses (Fig. 4, curves A′, B′, C′) for the three thicknesses are the same in the trachea. Proceeding distally, the net dose curves split, the largest (curve B′) and smallest (curve C′) net doses corresponding to the thinnest and thickest lining, respectively. At the 16th generation, they differ by a factor of about 1.5; from the first respiratory bronchioles (generation 17) to the pulmonary sacs, they differ by no more than a factor of 2.

Interspecies Comparison of Lower Respiratory Tract Dose Patterns

In Fig. 5A, B are plotted the LRT net and tissue dose curves for four species: rabbit, guinea pig, rat, and human. Depending on the particular anatomical model, the plots are dose versus zone (33, rabbit), order (69, guinea pig), and generation (80, human; 83, rat). Because of the construction of the anatomical models, it is not possible to have a one-to-one correspondence between the horizontal axis of a zone, order, or generation; thus, the four axes. However, we have matched those segments (the sequential groupings of airways, duct, and sacs as defined for the

particular model) that are equivalent. These include the tracheas, the last TB segments, the first RB in humans, and the first completely alveolated segments in the nonhuman species, and the last pulmonary segments.

The general shapes of the net dose curves (Fig. 5A) are the same, slowly decreasing distally in the TB region, with a more rapid decrease distally in the pulmonary region. There are differences in detail: the rat net dose peaks in the first segment of the pulmonary region, and the guinea pig net dose has a local maximum at this location. The net doses of both the human and rabbit continuously decrease, with no peak.

Tissue dose (Fig. 5B) is low in the trachea for all four species, being almost three orders of magnitude less than the tracheal net doses. Proceeding distally, the tissue doses increase to a maximum in the vicinity of the first segment in the pulmonary region and then decrease rapidly. The rabbit maximum occurs in the last segment of the TB region, whereas, the maximum guinea pig, rat, and human tissue doses occur in the first segment of the pulmonary region, a location where histopathological data show the major lesions in O_3 studies using monkeys (15) and rats (8).

The results shown in Fig. 5A, B were obtained with an appropriate URT model attached to each LRT anatomical model to take into account the effect of URT volume. However, no URT absorption was simulated. Accounting for URT absorption in each species would lower the predicted doses by an amount depending on each species' URT absorption and also, possibly, would put the curves in a vertical order different than plotted in Fig. 5. To make more definitive interspecies quantitative comparisons, URT removal must be considered.

Effect of the Tracheobronchial Region Liquid Lining Chemical Rate Constant on Ozone Uptake

The effect on regional and compartmental dose in rats and humans caused by different values of the TB liquid lining rate constant was investigated (Table 9). For the investigation, the anatomical models of Weibel (80) for humans and Yeh et al. (83) for rats were used. Three values of the rate constant were chosen: one-fifth the reference value, the reference value, and 5 times the reference value (i.e., the value based on reference material data) (48,58). Referring to Table 9, one can see that by increasing the rate constant of both species, the total uptakes, the total TB region uptakes, and the TB liquid lining uptakes increase, whereas the TB tissue uptakes and the pulmonary region uptakes decrease. The largest changes occur in the TB region, where the total rat TB tissue dose nearly triples and the TB tissue dose in humans increases by a factor of 2.5. On the other hand, the total LRT uptakes change by only a few percent, increasing 8% and 4.4% for the rat and human, respectively. The change in pulmonary tissue dose is larger, -19% and -31% for rats and humans, respectively.

The quantitative aspects of the changes illustrated in Table 9 in the percent uptakes

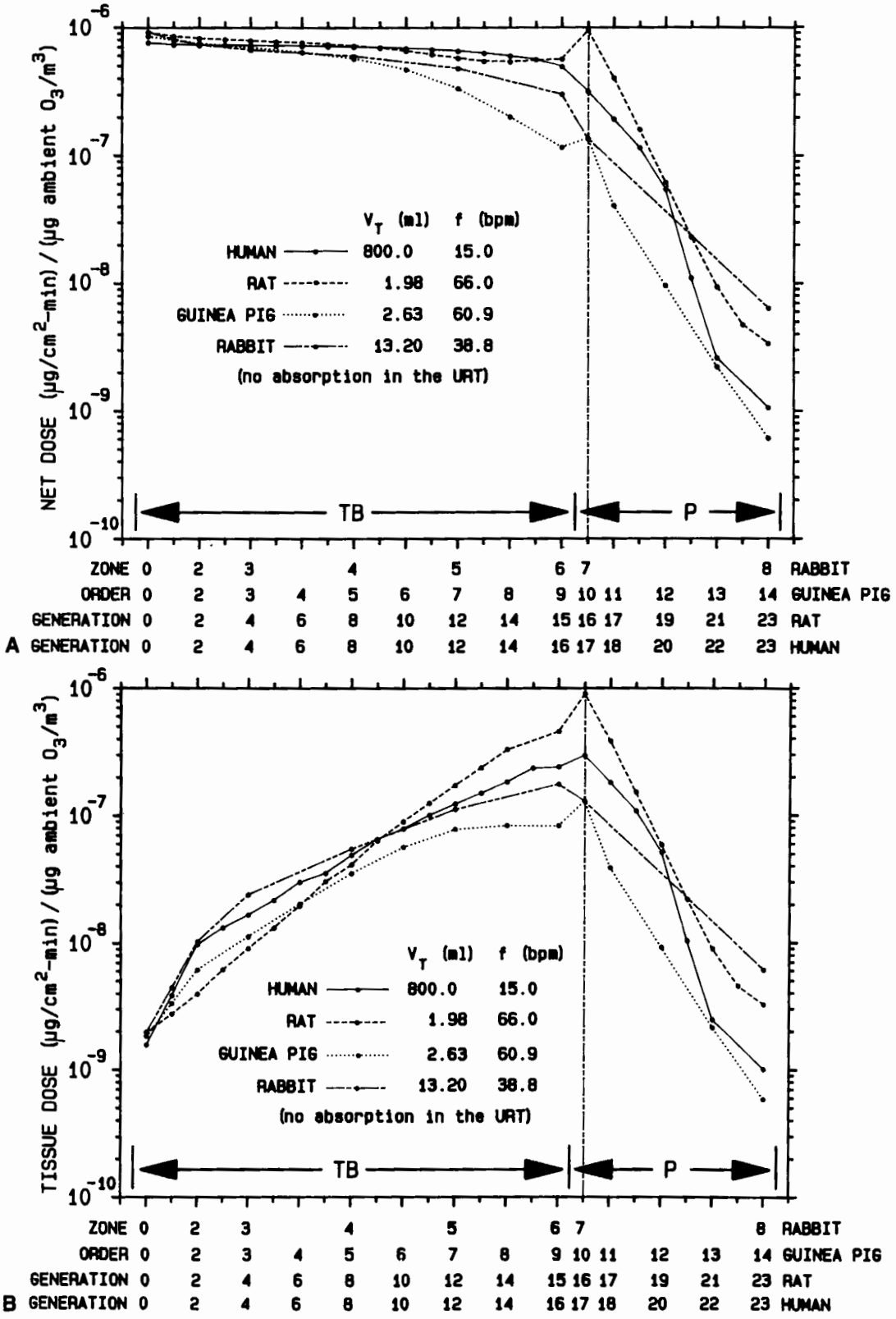

FIG. 5. Net dose (**A**) and tissue dose (**B**) versus sequential segments along anatomical model airway paths for human, rat, guinea pig, and rabbit. In general, each segment represents a group of airways or ducts, with common features as defined by the designers of the anatomical model (human and rat: generation; guinea pig: order; rabbit: zone). For a given species the plotted dots represent a predicted dose that corresponds to a given segment. The dots have been joined by lines for ease of interpreting the plots; these lines do not represent predicted values except where they intercept the dots. (From ref. 47.)

TABLE 9. *Effect of tracheobronchial liquid lining rate constant on the uptake of ozone in the regions and compartments of the lower respiratory tract of rat and human*[a]

	$(k_\mu/k_{\mu ref})$[b]	Total LRT uptake %	Tracheobronchial region uptake (%)			Pulmonary region uptake (%)[c]	
			Liquid lining	Tissue	Total TB	Tissue	Blood
Rat[d]	0.2	70.5	2.9	5.6	8.5	60.7	1.2
V_T = 2.40 ml	1.0	72.4	9.2	3.9	13.1	58.1	1.2
f = 81 bpm	5.0	76.4	22.6	1.6	24.2	51.1	1.0
Human	0.2	88.6	4.8	12.4	17.2	69.3	2.0
V_T = 800 ml	1.0	90.1	17.2	8.0	25.2	63.0	1.8
f = 15 bpm	5.0	92.5	41.3	1.9	43.2	47.8	1.4

[a]Uptake is the percentage of O_3 inhaled through the trachea that was absorbed by the region and compartment.
[b](k_μ) TB liquid lining rate constant; ($k_{\mu ref}$) reference TB liquid lining rate constant.
[c]Pulmonary liquid lining absorbs <0.1%.
[d]Rat data from ref. 58.

will depend on other factors in addition to the rate constant, including V_T and f. However, the qualitative aspects of the changes may be independent of these other parameter values; e.g., for the rat, Overton et al. (58) showed that for two values of the functional residual capacity and two sets of different ventilatory parameters, the qualitative aspects of uptake changes as a result of increasing the rate constant remained the same.

SUMMARY

In inhalation toxicology, an important concept involves the determination of dose as a major component for providing a perspective to judge the applicability of various toxicological results to human exposure conditions. We reviewed some of the biological, physical, and chemical factors that affect dose and that must be understood to interpret experimental toxicological data and to develop theoretical dosimetry models. Dosimetry experiments involving laboratory animals and humans were discussed, showing the variability in uptake according to the reactive gas, animal species, and respiratory tract region. The results of theoretical dosimetry models were illustrated, showing the effects on predictions due to different interspecies and intraspecies LRT anatomical models, due to different TB liquid lining thicknesses, and due to the chemical rate constant of the liquid lining of the TB region. Also illustrated was the use of predictions for interspecies dosimetry comparisons by comparing the dose profiles of rat, guinea pig, rabbit, and human. In spite of the complexities involved in experimental or theoretical dosimetry, results so far illustrate the feasibility of making interspecies LRT dosimetry comparisons for evaluating the toxicity of inhaled toxic gases, of providing sensitivity studies to determine processes and parameters needing additional research, and of assisting in experimental design.

ACKNOWLEDGMENT

The authors would like to express their appreciation to Andrew Barnett and Richard Graham for their excellent technical assistance and to Carolyn Wheeler for her excellent typing.

DISCLAIMER

The research described in this chapter has been reviewed by the Health Effects Research Laboratory, U.S. Environmental Protection Agency, and approved for publication. Approval does not signify that the contents necessarily reflect the views and policies of the Agency, nor does mention of trade names or commercial products constitute endorsement or recommendation for use.

REFERENCES

1. Adler, K. B., Wooten, O., and Dulfano, J. M. (1973): Mammalian respiratory mucociliary clearance. *Arch. Environ. Health*, 27:364–369.
2. Altman, P. L., and Dittmer, D. S. (1971): *Respiration and Circulation*. Federation of American Societies for Experimental Biology, Bethesda, MD.
3. Altman, P. L., and Dittmer, D. S., eds. (1974): *Biology Data Book, Vol. III*. Federation of American Society for Experimental Biology, Bethesda, MD.
4. Astarita, G. (1967): *Mass Transfer with Chemical Reaction*, p. 187. Elsevier, New York.
5. Bauer, M. A., Utell, M. J., Morrow, P. E., Speers, D. M., and Gibb, F. R. (1984): 0.30 ppm nitrogen dioxide inhalation potentiates exercise-induced bronchospasm in asthmatics. *Am. Rev. Respir. Dis.*, 129:A151.
6. Blackburn, F. L., Grant, J. P., and Young, V. R., eds. (1983): *Amino Acids (Metabolism and Medical Applications)*. John Wright, London.
7. Boat, T. F., and Cheng, P. W. (1980): Biochemistry of airway mucus secretions. *Fed. Proc.*, 39:3067–3074.
8. Boorman, G. A., Schwarts, L. W., and Dungworth, D. L. (1980): Pulmonary effects of prolonged ozone insult in rats. *Lab. Invest.*, 43(2):108–115.
9. Clements, J. A., and King, R. J. (1976): *The Biochemical Basis of Pulmonary Function*, edited by R. G. Crystal, pp. 143–150. Dekker, New York.
10. Clever, H. L., and Battino, R. (1975): The solubility of gases in liquids. In: *Solutions and Solubilities*, edited by M. R. J. Dack, pp. 379–385. Wiley, New York.
11. Corn, M., Kotscko, N., and Stanton, D. (1976): Mass transfer coefficient for sulphur dioxide and nitrogen dioxide removal in cat upper respiratory tract. *Ann. Occup. Hyg.*, 19:1–12.
12. Crapo, J. D., Young, S. L., Fram, E. K., Pinkerton, K. E., Barry, B. E., and Crapo, R. O. (1983): Morphometric characteristics of cells in the alveolar region of mammalian lungs. *Am. Rev. Respir. Dis.*, 128:542–546.
13. Creeth, M. M., Bhaskar, K. R., and Horton, J. R. (1977): The separation and characterization of bronchial glycoproteins by density-gradient methods. *Biochem. J.*, 167:557–569.
14. Danckwerts, F. R. S. (1970): *Gas–liquid Reactions*. McGraw-Hill, New York.
15. Dungworth, D. L., Castleman, W. L., Chow, C. K., et al. (1975): Effect of ambient levels of ozone on monkeys. *Fed. Proc.*, 34:1670–1674.
16. Durham, J. D., Barnes, H. M., and Overton, J. H. Jr. (1984): Acidification of rain by oxidation of dissolved sulfur dioxide and the absorption of nitric acid. In: *Chemistry of Particles, Fogs and Rain, Vol. 2*, edited by J. L. Durham, pp. 197–236. Butterworth, Boston.
17. Durham, J. L., Overton, J. H. Jr., and Aneja, V. P. (1981): Influence of gaseous nitric acid on sulfate production and acidity in rain. *Atmos. Environ.*, 15:1059–1068.
18. Engle, J. L. (1972): Retention of inhaled formaldehyde, propionaldehyde, and acrolein in the dog. *Arch. Environ. Health*, 25:119–124.
19. Environmental Protection Agency. (1978): Toxicological appraisal of photochemical oxidants. In: *Air Quality Criteria for Ozone and Other Photochemical Oxidants*, Chap. 8, pp. 136–199. U.S. Government Printing Office, Washington, DC.
20. Farrell, P. M. (ed.) (1982): *Lung Development: Biochemical and Clinical Perspectives (Biochemistry and Physiology). Vol. I*. Academic Press, New York.
21. Fasman, G. D. (ed.) (1976): *Handbook of Biochemistry and Molecular Biology*. CRC Press, Boca Raton, FL.
22. Felicetti, S. A., Wolff, R. K., and Muggenburg, B. A. (1981): Comparison of tracheal mucous transport in rats, guinea pigs, rabbits and dogs. *J. Appl. Physiol.*, 51(6):1612–1617.
23. Fiserova-Bergerova, F. (1983): *Modeling of Inhalation Exposure to Vapors: Uptake, Distribution, and Elimination. Vols. I and II*. CRC Press, Boca Raton, FL.
24. Gerrity, T. R., Weaver, R. A., Berntsen, J., House, D. E., and O'Neil, J. J. (1988): Extrathoracic and intrathoracic removal of ozone in tidal breathing humans. *J. Appl. Physiol.* (in press).
25. Gier, J. de, van Deenen, L. L. M., Verlop, M. C., and van Gastel, L. (1964): Phospholipid and fatty acid characteristics of erythrocytes in some cases of anaemia. *Br. J. Haematol.*, 10:246–256.
26. Goldstein, E., Hackney, J. D., and Stanley, N. R. (1985): Photochemical air pollution. Part I. (Specialty Conference). *West J. Med.*, 142:369–376.
27. Hales, J. M., and Sutter, S. L. (1973): Solubility of sulfur dioxide in water at low concentrations. *Atmos. Environ.*, 1:997–1001.

28. Hallgren, B., Stenhagen, S., Svanborg, A., and Svennerholm, L. (1960): Fatty acid composition of plasma lipids in normals and diabetics. *J. Clin. Invest.*, 39:1424–1434.
29. Heck, H. d'A., Chin, T. Y., and Schmitz, M. C. (1983): Distribution of [^{14}C] formaldehyde in rats after inhalation exposure. In: *Formaldehyde Toxicity*, edited by J. E. Gibson, pp. 26–37. Hemisphere Publishing Corporation, Washington, DC.
30. Horimoto, M., Koyama, T., Kikuchi, Y., Kakiuchi, Y., and Murao, M. (1981): Effect of trans-pulmonary pressure on blood-flow velocity in pulmonary micro-vessels. *Respir. Physiol.*, 43:31–41.
31. Hulbert, W. C., Forster, B. B., Laird, W., Phil, C. E., and Walter, D. C. (1982): An improved method for fixation of the respiratory epithelial surface with the mucous and surfactant layers. *Lab. Invest.*, 47:354–363.
32. Iravani, J., and van As, A. (1972): Mucus transport in the tracheobronchial tree of normal and bronchitic rats. *J. Pathol.*, 106:81–93.
33. Kliment, V. (1973): Similarity and dimensional analysis, evaluation of aerosol deposition in the lungs of laboratory animals and man. *Folia Morphol.*, 21:59–64.
34. Köhler, H. P., Kolssek, H., Aurich, B. and Strobel, H. (1969): Der Gehalt des menschlichen bronchial sekretes on foreign aminosauren. *Z. Erk. Atmungsorgane*, 130:259–265.
35. Lechnenger, A. L. (1975): *Biochemistry*. Worth Publishers, New York.
36. Lee, Y.-N., and Schwartz, S. E. (1981): Reaction kinetics of nitrogen dioxide with liquid water at low partial pressure. *J. Phys. Chem.*, 85(7):840–848.
37. Lewis, R. W. (1971): Lipid composition of human bronchial mucus. *Lipids*, 6:859–861.
38. Lopez-Vidriero, M. T., and Reid, L. (1980): Respiratory tract fluids—Chemical and physical properties of airway mucus. *Eur. J. Respir. Dis.* (Suppl), 110:21–26.
39. Lucas, A. M., and Douglas, L. C. (1934): Principles underlying ciliary activity in the respiratory tract. *Arch. Otolaryngol.*, 20:528–541.
40. Luchtel, D. L. (1976): Ultrastructural observations on the mucous layer in pulmonary airways ICCB Abstract No. 1048. *J. Cell. Biol.*, 70:350a.
41. Luchtel, D. L. (1978): The mucus layer of the trachea and major bronchi in the rat. *Scan. Electron Microsc.*, 11: 1089–1098.
42. Martonen, T. B., Barnett, A. E., and Miller, J. J. (1985): Ambient sulfate aerosol deposition in man: Modeling the influence of hygroscopicity. *Environ. Health Perspect.*, 63:11–24.
43. Menzel, D. B. (1976): The role of free radicals in the toxicity of air pollutants (nitrogen dioxide and ozone). In: *Free Radicals in Biology, Vol. 11*, edited by W. A. Pryor, pp. 181–202. Academic Press, New York.
44. Menzel, D. B. (1984): Ozone: An overview of its toxicity in man and animals. In: *Fundamentals of Extrapolation Modeling of Inhaled Toxicants: Ozone and Nitrogen Dioxide*, edited by F. J. Miller and D. B. Menzel, pp. 3–4. Hemisphere, Washington, DC.
45. Miller, J. J., McNeal, C. A., Kirtz, J. M., Gardner, D. E., Coffin, D. L., and Menzel, D. B. (1979): Nasopharyngeal removal of ozone in rabbits and guinea pigs. *Toxicology*, 14:272–281.
46. Miller, F. J., Menzel, D. B., and Coffin, D. L. (1978): Similarity between man and laboratory animals in regional pulmonary deposition of ozone. *Environ. Res.*, 17:84–101.
47. Miller, F. J., Overton, J. O., Gerrity, T. R., and Graham, R. C. (1987): Interspecies dosimetry of reactive gases. In: *Proceedings of The Design and Interpretation of Inhalation Studies and Their Use in Risk Assessment*, Hannover, W. Germany, March 23–27, 1987.
48. Miller, F. J., Overton, J. H., Jr., Jaskot, R. H., and Menzel, D. B. (1985): A model of the regional uptake of gaseous pollutants in the lung. I. The sensitivity of the uptake of ozone in the human lung to lower respiratory tract secretions and exercise. *Toxicol. Appl. Pharmacol.*, 79:11–27.
49. Miller, F. J., Overton, J. H., Smolko, E. D., Graham, R. C., and Menzel, D. B. (1987): *Hazard Assessment Using an Integrated Physiologically Based Dosimetry Modeling Approach: Ozone*. National Academy of Sciences, Washington, DC.
50. Moorman, W. J., Chmiel, J. J., Stara, J. F., and Lewis, T. R. (1973): Comparative decomposition of ozone in the nasopharynx of beagles. Acute vs. chronic exposure. *Arch. Environ. Health*, 26:153–155.
51. Morgan, K. T., Jrang, X-Z, Patterson, D. L., and Gross, E. A. (1984): The nasal mucociliary apparatus. *Am. Rev. Respir. Dis.*, 130:275–281.
52. Morrow, P. E. (1986): Personal communication. Department of Radiation Biology and Biophysics. The University of Rochester, School of Medicine and Dentistry, Rochester, NY 14642.
53. National Research Council. (1977): *Committee on Medical and Biologic Effects of Environmental*

Pollutants, Subcommittee on Ozone and Other Photochemical Oxidants. Toxicology, Ozone and Other Photochemical Oxidants, pp. 323–387. National Academy of Sciences, Washington, DC.
54. Navari, R. M., Gainer, J. L., and Hall, K. R. (1971): A predictive theory for diffusion in polymer and protein solutions. *AlChE J.*, 17(5):1028–1036.
55. Nelson, G. J. (ed.). (1972): *Blood Lipids and Lipoproteins*, p. 980. Wiley-Interscience, New York.
56. Overholser, K. A., Bhattacharya, J., and Staub, N. C. (1981): Microvascular pressures in the isolated, perfused dog lung: Comparison between theory and measurement. *Microvasc. Res.*, 23:67–76.
57. Overton, J. H. Jr. (1984): Physicochemical processes and the formulation of dosimetry models. *J. Toxicol. Environ. Health*, 13(2–3):273–294.
58. Overton, J. H., Graham, R. C., and Miller, F. J. (1987): A model of the regional uptake of gaseous pollutants in the lung. II. The sensitivity of ozone uptake in laboratory animal lungs to anatomical and ventilatory parameters. *Toxicol. Appl. Pharmacol.*, 88:418–432.
59. Overton, J. H., Graham, R. C., and Miller, F. J. (1987): *Mathematical Modeling of Ozone Absorption in the Lower Respiratory Tract*. National Academy of Sciences, Washington, DC.
60. Passero, M. A., Tye, R. W., Kilburn, K. H., and Linn, W. S. (1973): Isolation and characterization of two glycoproteins from patients with alveolar proteinosis. *Proc. Natl. Acad. Sci. USA*, 70:973–976.
61. Perry, R. H., Chilton, C. H., and Kirkpatrick, S. D. (eds.). (1963): *Chemical Engineers Handbook, 4th ed.* McGraw-Hill, New York.
62. Phillips, G. B., and Dodge, J. T. (1967): Composition of phospholipids and of phospholipid fatty acids of human plasma. *J. Lipid Res.*, 8:676–681.
63. Postlethwait, E. M., and Mustafa, M. G. (1981): Fate of inhaled nitrogen dioxide in isolated perfused rat lung. *J. Toxicol. Environ. Health*, 7:861–872.
64. Proctor, D. F. (1982): The mucociliary system. In: *The Nose. Upper Airway Physiology and the Atmospheric Environment*, edited by D. F. Proctor and I. Anderson, pp. 245–278. Elsevier Biomedical Press, Amsterdam.
65. Pryor, W. A., Dooley, M. M., and Church, D. F. (1983): Mechanism for the reaction of ozone with biological molecules: The source of the toxic effects of ozone. *Adv. Mod. Environ. Toxicol.*, 5:7–19.
66. Razumovskii, S. D., and Zaikov, G. E. (1972): Effect of structure of an unsaturated compound on rate of its reaction with ozone. *J. Gen. Chem. USSR*, 8 (3):464–468.)
67. Sahu, S., and Lynn, W. S. (1977): Lipid composition of secretions from patients with asthma and patients with cystic fibrosis. *Am. Rev. Respir. Dis.*, 115:233–239.
68. Sahu, S., and Lynn, W. S. (1979): Characterization of a high-molecular-weight glycoprotein isolated from the pulmonary secretions of patients with alveolar proteinosis. *Biochem. J.*, 177:153–158.
69. Schreider, J. P., and Hutchens, J. O. (1980): Morphology of the guinea pig respiratory tract. *Anat. Rec.*, 196:313–321.
70. Sherwood, T. K., Pigford, R. L., and Wilke, S. (1975): *Mass Transfer*. McGraw-Hill, New York.
71. Stephens, R. J., Sloan, M. F., Evans, M. J., and Freeman, G. (1974): Early response of lung to low levels of ozone. *Am. J. Pathol.*, 74:31–58.
72. Stuart, B. O. (1984): Deposition and clearance of inhaled particles. *Environ. Health Perspect.*, 55:369–390.
73. Swenberg, J. A., Gross, E. A., Martin, J., and Popp, J. A. (1983): Mechanisms of formaldehyde toxicity. In: *Formaldehyde Toxicity*, edited by J. E. Gibson, pp. 26–37. Hemisphere, Washington, DC.
74. Van As, A. (1977): Pulmonary airway clearance mechanisms: A reappraisal. *Am. Rev. Respir. Dis.*, 115:721–726.
75. Van As, A., and Webster, I. (1972): The organization of ciliary activity and mucus transport in pulmonary airways. *S. Afr. Med. J.*, 46:347–350.
76. Van As, A., and Webster, I. (1974): The morphology of mucus in mammalian pulmonary airways. *Environ. Res.*, 7:1–12.
77. Vaughan, R. R. Jr., Jennelle, L. F., and Lewis, T. R. (1969): Long-term exposure to low levels of air pollutants. Effects on pulmonary function in the beagle. *Arch. Environ. Health*, 19:45–50.
78. Velasquez, D. J., and Morrow, P. E. (1984): Estimation of guinea pig tracheobronchial transport rates using a compartmental model. *Exp. Lung Res.*, 7:163–176.
79. Wagner, W. W. Jr., Latham, L. P., Gillespie, M. N., and Guenther, J. P. (1982): Direct measurements of pulmonary capillary transit times. *Science*, 218:379–381.

80. Weibel, E. R. (1963): *Morphometry of the Human Lung*. Academic Press, New York.
81. Weibel, E. R. (1973): Morphological basis of alveolar–capillary gas exchange. *Physiol. Rev.*, 53(2):419–495.
82. Wiester, M. J., Williams, T. B., King, M. E., Ménache, M. G., and Miller, F. J. (1987): Ozone uptake in awake Sprague-Dawley rats. *Toxicol. Appl. Pharmacol.*, 89:429–437.
83. Yeh, H. C., Schum, G. M., and Duggan, M. T. (1979): Anatomic models of the tracheobronchial and pulmonary region of the rat. *Anat. Rec.*, 195:483–492.
84. Yokoyama, E., and Frank, R. (1972): Respiratory uptake of ozone in dogs. *Arch. Environ. Health*, 25:132–138.
85. Yoneda, K. (1976): Mucous blanket of rat bronchus. *Am. Rev. Respir. Dis.*, 114:837–842.
86. Zhuang, F. Y., Fung, Y. C., and Yen, R. T. (1983): Analysis of blood flow in cat's lung with detailed anatomical and elasticity data. *J. Appl. Physiol.*, 55(4):1341–1348.